Model of metallic filament formation and rupture in NiO for unipolar switching

Hyung Dong Lee, Blanka Magyari-Köpe, and Yoshio Nishi
Department of Electrical Engineering, Stanford University, Stanford, California 94305, USA
(Received 17 February 2010; published 12 May 2010)

The structural and electronic implications of cation and anion vacancies in NiO are assessed using density functional theory in conjunction with the local-density approximation and employing on-site Coulomb corrections within the LDA+U method. Electronic band-structure data supports the p-type semiconducting oxide character. The calculated formation energies identify the stability of charged vacancy states consistent with experimental reports. We present a microscopic model for the formation and rupture of an electrically active filament in NiO targeted to explain the unipolar switching phenomenon observed in resistive change memory devices. The formation and filament rupture processes are linked to the migration of oxygen in the oxide coupled with the oxidation/reduction process of nickel atoms.

DOI: 10.1103/PhysRevB.81.193202 PACS number(s): 71.30.+h, 71.20.Be, 71.15.Mb

Resistance change random access memory (ReRAM) based on transition-metal oxides (TMOs) such as NiO, TiO_2 had been extensively investigated as candidates for the next generation of memory devices, due to their simplicity in composition and scaling capability in the future.[1,2] Even though the switching phenomena had been observed in various materials, the fundamental understanding of the switching mechanism and its physical origin is still lacking. It had been suggested from experiments, that the so-called "filament model" gives a qualitative explanation for the unipolar switching in NiO ReRAM; i.e., a conductive path called filament is formed and ruptured by the applied electrical stress, a process performed repeatedly.[3] Nevertheless, the microscopic understanding of the filament is still in question. In the last years different models had been proposed for the filament formation.[4,7,14] It has been suggested that the metallic Ni defects in NiO film may be responsible for the filament channel[5] and that the metallic defects are due to injected metal ions from anode to the insulator.[4] "On" and "off" states were interpreted as charging and discharging electronic states due to metallic defects.[1,4] However, there are additional experimentally observed facts associated with the switching, i.e., oxygen migration,[6] thermal energy considerations,[7,8] crystal disorder, electrode interface effects,[9] etc. Also, it has been shown that defects in TMO may change conductivity drastically.[10] Concentration or distribution of vacancy defects may vary during the "on" and "off" transitions due to atomic migration.

In this Brief Report, we discuss a model for the filament formation and rupture based on first-principles calculations using density functional theory. We consider several charged cation and anion vacancy defects and determine their stability as a function of the Fermi energy. Then, we assess the structural and electronic implications of a filament composed of oxygen vacancy chains.

The electronic structure calculations were performed using the VASP code.[11] The projector-augmented-wave pseudopotentials[12,13] are used for nickel and oxygen with valence configurations of $3d^8 4s^2$ and $2s^2 2p^4$, respectively. Spin-polarized generalized gradient approximations (SGGAs) in conjunction with the Hubbard-type on-site Coulomb corrections has been found to describe accurately NiO by taking into account the strong electronic correlations between $3d$ electrons.[14] $U=6.3$ and $J=1$ were used to describe the on-site interactions within the rotationally invariant SGGA+U method.[15] The obtained bulk properties for NiO are in very good agreement with experiments, i.e., lattice constant 4.21 Å (4.19),[16,17] bulk modulus 188.55 GPa (205),[17] energy gap 3.256 eV (4),[17,18] and magnetic moment $1.671\mu_B$ (1.64) (Refs. 18 and 19); the values in parentheses are experimental.

A supercell containing 128 atoms, $Ni_{64}O_{64}$ was used for both single vacancy and multi vacancy studies as shown in Fig. 1(a) rather than rock salt structure as in Fig. 1(b) to use the reduced number of atoms in calculations. Electronic wave functions were expanded with a plane-wave energy cutoff of 500 eV. K points in Brillouin zone is sampled with a $2\times2\times2$ k points by the Monkhorst-Pack scheme. All atoms were relaxed using conjugated gradient method until Hellmann-Feynman forces on each atom are reduced to 0.05 eV/Å.

Partial density of states (PDOS) of nickel $3d$ and oxygen $2p$ orbital of relaxed NiO supercell with single cation or anion vacancy is shown as a function of the charge state of the vacancy in Figs. 1(c) and 1(d). The states at valence-band maximum (VBM) are composed of the mixture of nickel $3d$ and oxygen $2p$ orbital and states at conduction-band minimum (CBM) are of only nickel $3d$ orbital as shown in Figs. 1(c) and 1(d).[15] The energy-band diagram shows the position of several defect states in the band gap. Defect states in solid shape refer to the occupied states and states in empty shape to empty states. Energy level of zero represents VBM and the horizontal mark refers to the CBM in Figs. 1(e) and 1(f). The energy-band gap depends on the charge state of anion/cation vacancies suggesting that electrons in conduction band or holes in valence band may experience more scattering in nonstoichiometric TMO. For cation vacancy, band gap varies from 3.14 eV, 3.26 eV, and 3.41 eV according to charge state of −2 to 0 with a change by −3.5%, 0.1%, and 4.7% from bulk, respectively. For anion vacancy, band gap has a change by 12.4%, 9%, and 4.7% from bulk with charge state of 0 to 2.

NiO has been found to be mostly a Ni-deficient oxide; however, if oxygen vacancies are also present, they can provide electrons to surrounding Ni atoms, as indicated by the fact that the lowest localized band-gap states are occupied by electrons in Fig. 1(f). However, electrons which are expected to mostly distribute over six 1 NN Ni atoms may redistribute

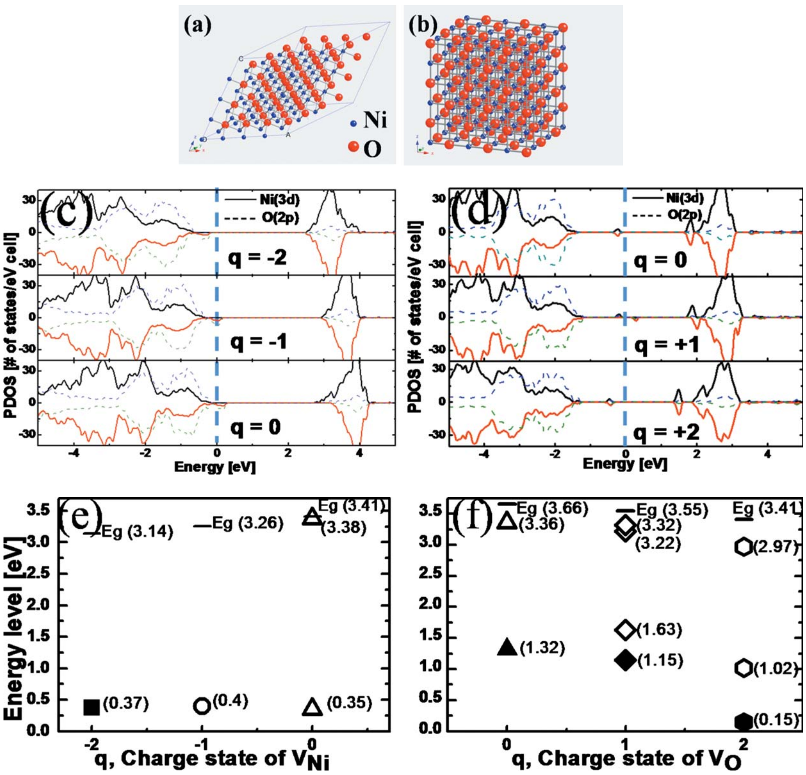

FIG. 1. (Color online) Supercell of (a) $Ni_{64}O_{64}$ and of (b) NiO in simple-cubic NaCl structure. Partial density of states (Ni 3*d* and O 2*p*) and energy-band diagram showing the defect energy levels (c) and (e) for V_{Ni} and (d) and (f) for V_O. Fermi level is set to 0 eV (c) and (d). CBM is composed of Ni 3*d* orbital and VBM is of the mixture of Ni 3*d* and O 2*p* orbital in all calculations as shown in (c) and (d). The occupied lowest defect states in (f) come from first nearest neighbor (1 NN) Ni 3*d*, 1 NN Ni 3*d* +O 2*p*, and 1 NN O 2*p* orbital from oxygen vacancy site according to vacancy charge state 0 to 2. Defect states with filled symbols refer to the occupied states, while unfilled symbols represent empty states.

onto only one surrounding Ni atom as shown in Fig. 4(b).

In order to assess electron transition states we have calculated the stability of the vacancy charge states. The formation energies are shown in Fig. 2. They were determined for each charge state of cation and anion vacancies using the following equation:

$$E_{\text{form}}{}^{q} = E(V_N{}^{q}) - \text{E(perfect)} + n_{Ni}\mu_{Ni} + n_O\mu_O + \text{q}(E_F + \text{VBM}^{+q})$$

where $E(V_N{}^q)$ and E(perfect) are total energies of a supercell with and without defects for charge state q, respectively. n_{Ni} and n_O represent the number of the removed Ni and O atoms. μ_{Ni} and μ_O refer to the atomic chemical potentials of Ni and O. E_F is the Fermi level with respect to VBM.

With the Fermi level in the vicinity of VBM due to *p*-type semiconducting property, the stable oxygen vacancy state is positively charged (+2), then a transition to neutral charge state is observed at 0.95 eV and finally the singly negatively charged vacancy state is stabilized above 2.83 eV. In contrast, for the case of Ni vacancies, several charge states (−2, −1, 0) may coexist since formation energies for those vacancies are comparable when Fermi level is close to VBM.

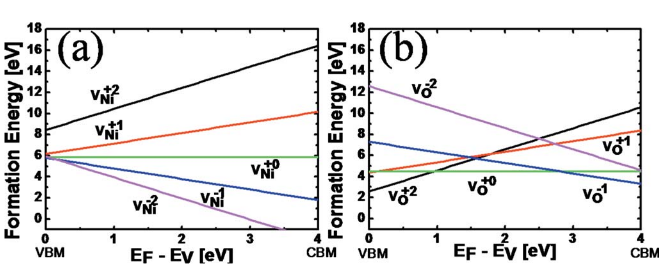

FIG. 2. (Color online) Formation energy of charged vacancies (a) for V_{Ni} and (b) for V_O

In vacancy-rich TMOs, the generated local electric field may act as a scattering source, which makes electrons or holes localized/trapped in vacancy sites. The as-deposited NiO films show *p*-type conductivity because they are mainly grown with Ni deficiency. In Fig. 1(e), most of the defect levels are near the VBM in the range of 0.37 eV for all negatively charged and neutral Ni vacancies. Ionization energies are determined from Fig. 2(a); i.e., the transition states at which the charged Ni vacancies become stable, −0.04 eV for $q=-1$ and 0.16 eV for $q=-2$. These low energies for acceptorlike states support the possibility of *p*-type conductivity in Ni-deficient NiO films observed in experiments.[20]

The formation energies of an oxygen vacancy in the proximity of VBM are lower than that of the nickel vacancies in good agreement with Ref. 15. However, the −2 charge Ni vacancy becomes increasingly more stable as the Fermi level approaches the CBM.

We present a microscopic model of filament formation and rupture by employing the stable vacancy states determined in earlier calculations. The schematic of filament formation and rupture in a microscopic view is shown in Fig. 3. Figures 3(a) and 3(b) are about formation and rupture mechanism, respectively. The resultant states after formation/rupture of filament are shown in Figs. 3(c) and 3(d). High electric fields during the so-called "forming process" or at the "on" transition may cause the migration of oxygen through the device.[6,25] In general the removal of an oxygen atom creates an oxygen vacancy of +2 charge and 2 electrons which become localized on the nearby Ni atoms.[15] Considering a Ni atom in the proximity of these oxygen vacancies the charge state of this Ni atom may turn Ni^{2+} (approx. the

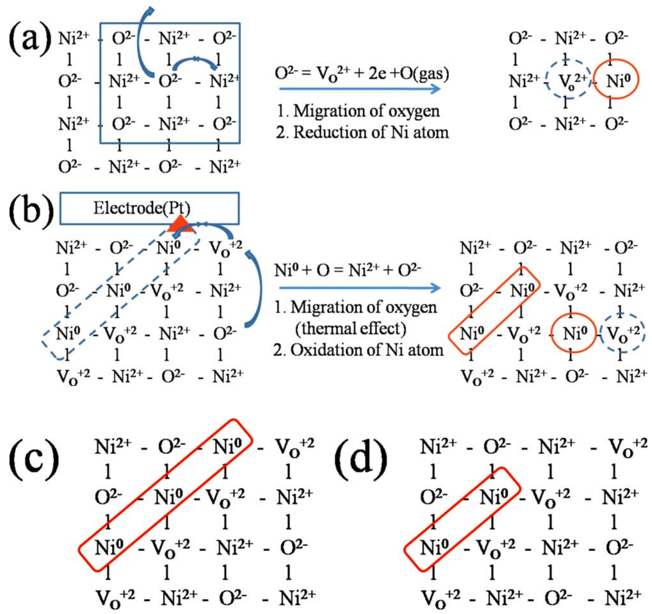

FIG. 3. (Color online) (a) Formation and (b) rupture mechanism in a microscopic view and its corresponding states to (c) formation and (d) rupture of metallic filament

charge state of Ni in bulk NiO) into Ni^{1+} or Ni^0. Hickmott *et al.* had pointed out that the states formed by neutral nickel defects are placed at midgap and play an important role in switching by charging or discharging the states.[1,21] However, the formation of metallic defects certainly requires strong impulse such as relatively large local structural deformation, the presence of several oxygen vacancies and/or migration of metal atoms. Our model is based on the assumption that the migration of oxygen has taken place as observed in recent experiments.[22,25] We consider that the oxygen vacancies are formed during the deposition under certain growth conditions[1,3,4] and much more during the forming process by strong electrical impulses since they have lower formation energy than Ni vacancies.

During the forming process, a high electric field is applied and oxygen ions participating in Ni-O bonds may migrate resulting in +2 oxygen vacancy, stable charge state as determined earlier, and two electrons to be used in the reduction of nickel atom [Fig. 3(a)]. They tend to cluster in certain configurations with lower V_o-V_o interactions.[15,27,28] As a result, metallic nickel atoms are connected in a chain as shown in Fig. 3(c). Thus, the so formed atomic chain can be regarded as a metallic filament representing the "on" state.

The current density through a metallic filament has been shown to reach high values and might be responsible for generating the thermal energy that will activate the migration of oxygen at the highest resistive point or at electrode-filament interface.[23] Then, the rupture process of the metallic filament as shown in Fig. 3(b) is due to oxygen migration[24] to oxygen vacancy sites near chainlike metallic nickel atoms away from the filament and oxidation of those nickel atoms to recover their bulklike oxygen coordination. The recovery of oxygen coordination of nickel atoms connected in a chain can be regarded as rupture of filament representing the "off" state as shown in Fig. 3(d).

Our model of the filament structure is supported by observations of a neutral metallic peak with x-ray photoelectron spectroscopy in all NiO films that show the switching behavior.[25] Experimental evidence has also been presented for the oxygen vacancy migration after the forming process.[25]

The filament structure considered here contains four Ni atoms in each unit cell; of which two equivalent Ni atoms are surrounded by four oxygen vacancies, while the other two Ni atoms have only two nearest neighboring oxygen vacancies. The filament has an alternating higher/lower electronic charge density distribution along the $\langle 110 \rangle$ direction, depending on the oxygen vacancy concentration. The electronic charge distribution around nickel atoms was calculated for the supercell with the oxygen vacancies around the metallic filament. The (100) plane with six oxygen vacancies, shown in Fig. 4(a) is one of the configurations with the lowest formation energy, in agreement with Ref. 12. The filament is in the $\langle 110 \rangle$ direction. Bader charge analysis[26] had been performed to investigate the amount of charge belonging to each nickel atom in a filament. We find that the charges for the four nickel atoms along the filament [Fig. 4(a)] are increased compared to the charge of $8.68e$ for nickel in perfect NiO, that is, 9.1 and 9.8 depending on the oxygen vacancy coordination around each Ni atom, as shown in Fig. 4(a). Both types of nickel atoms show almost neutral atomic character implying that the removal of several oxygen atoms can generate almost neutral metallic defects, Ni^0. The Bader volume (radius) of the four nickel atoms along the filament path is also larger by 80.5% (1.23 times) compared with that of nickel atom in bulk NiO. The electrons are spread around the Ni atoms resulting in charge is redistributed around the Ni atoms when the filament is formed.

To investigate the effect of the filament formation on the electronic structure, the density of states of the supercell has been calculated [Fig. 4(c)]. Defect levels are distributed over the whole range of the forbidden gap and NiO becomes metallic. We calculate the PDOS of each nickel atom to understand its contributions to the electronic transport. All the states near or below Fermi level are from nickel atoms further away from the filament. The transport would be similar to polaron hopping, which could be dominant in "off" state or in as-deposited film. This effect is in good agreement with experimental results of Jung *et al.*;[29] where a coexist of weak metallic conduction and polaron hopping in high resistance state is proposed. The states just above Fermi level and below CBM correspond to nickel atoms in the filament [Figs. 4(b) and 4(d)–4(f)]. The calculation has been done at $T = 0$ K, electrons at room temperature can populate the states above Fermi level and the filament will contribute to the observed higher conductivity. Figure 4(b) shows band decomposed (partial) charge density within $E_F \sim E_F + 0.3$ eV suggesting transport path is in a direction of filament. A more thorough examination on the electronic transport in this system may help us understand the effect of temperature on both the transport of electrons in the filament and migration of oxygen atoms.

In conclusion we presented a model for the formation and rupture mechanism in NiO, a microscopic view for the unipolar switching in NiO, which agrees with existing experi-

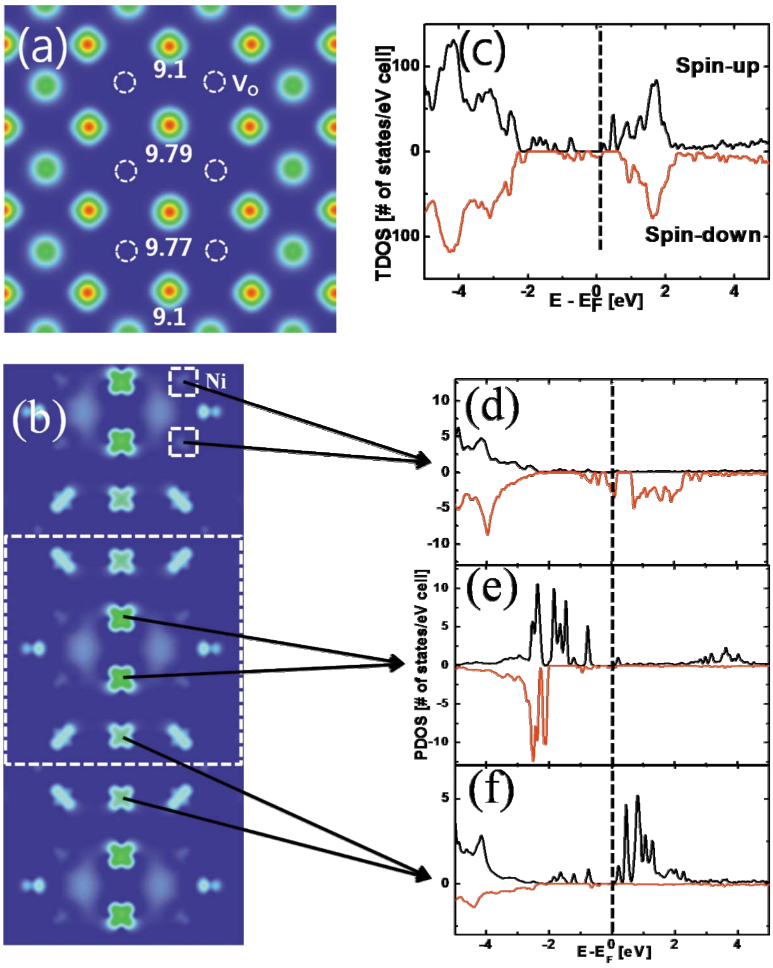

FIG. 4. (Color online) (a) Charge density of supercell with six oxygen vacancies and (b) partial charge density within $E_F \sim E_F + 0.3$ eV in (100) plane including oxygen vacancies and Ni metal chain. (c) Total density of states of the supercell and (d)–(f) partial density of states of d orbitals at each Ni atom. Fermi level is set to 0 eV (c)–(f). Dotted circle in (a) refers to oxygen vacancy site and square in (b) to Ni site. The number located at each Ni atom of the filament in (a) represents charge from Bader charge analysis; 8.68*e* for Ni and 7.32*e* for O in perfect NiO.

mental observations. The formation process of a metallic filament is regarded as a two-step process: (1) migration of oxygen vacancies by the applied high electric field in the "forming process" or at the "on" transition and (2) reduction in nickel atoms in the proximity of oxygen vacancies. The rupture process can be seen as migration of oxygen vacancies away from the filament and oxidation of nickel atom to recover their bulklike coordination.

The computational work was carried out through the National Nanotechnology Infrastructure Network's Computational cluster at Stanford University, NMTRI.

[1] S. Seo *et al.*, Appl. Phys. Lett. **85**, 5655 (2004).
[2] C. Rohde *et al.*, Appl. Phys. Lett. **86**, 262907 (2005).
[3] B. J. Choi *et al.*, J. Appl. Phys. **98**, 033715 (2005).
[4] M. J. Lee *et al.*, J. Appl. Phys. **103**, 013706 (2008).
[5] J. G. Simmons and R. R. Verderber, Proc. R. Soc. London, Ser. A **301**, 77 (1967).
[6] H. Tang, F. Li, and J. Shinar, Appl. Phys. Lett. **71**, 2560 (1997).
[7] J. F. Gibbons and W. E. Beadle, Solid-State Electron. **7**, 785 (1964).
[8] Y. Sato *et al.*, Appl. Phys. Lett. **90**, 033503 (2007).
[9] C. Park *et al.*, Appl. Phys. Lett. **93**, 042102 (2008).
[10] J. B. Torrance, Physica C **182**, 351 (1991).
[11] G. Kresse and J. Hafner, Phys. Rev. B **47**, 558(R) (1993); **49**, 14251 (1994).
[12] P. E. Blöchl, Phys. Rev. B **50**, 17953 (1994).
[13] J. P. Perdew, K. Burke, and M. Ernzerhof, Phys. Rev. Lett. **77**, 3865 (1996).
[14] A. Rohrbach, J. Hafner, and G. Kresse, Phys. Rev. B **69**, 075413 (2004).
[15] S. Park *et al.*, Phys. Rev. B **77**, 134103 (2008).
[16] W. E. Pickett, S. C. Erwin, and E. C. Ethridge, Phys. Rev. B **58**, 1201 (1998).
[17] S. L. Dudarev *et al.*, Phys. Rev. B **57**, 1505 (1998).
[18] O. Bengone *et al.*, Phys. Rev. B **62**, 16392 (2000).
[19] S. V. Faleev, M. van Schilfgaarde, and T. Kotani, Phys. Rev. Lett. **93**, 126406 (2004).
[20] A. J. Bosman, H. J. Van Daal, and G. F. Knuvers, Phys. Lett. **19**, 372 (1965).
[21] W. R. Hiatt and T. W. Hickmott, Appl. Phys. Lett. **6**, 106 (1965).
[22] K. Kinoshita *et al.*, Appl. Phys. Lett. **89**, 103509 (2006).
[23] U. Russo *et al.*, IEEE Electron Device Lett. **30**, 817 (2009).
[24] H. Shima *et al.*, Appl. Phys. Lett. **91**, 012901 (2007).
[25] M.-J. Lee *et al.*, Nano Lett. **9**, 1476 (2009).
[26] G. Henkelman, A. Arnaldsson, and H. Jónsson, Comput. Mater. Sci. **36**, 354 (2006).
[27] D. I. Woodward *et al.*, Appl. Phys. Lett. **84**, 4650 (2004).
[28] D. A. Muller *et al.*, Nature (London) **430**, 657 (2004).
[29] K. Jung *et al.*, Appl. Phys. Lett. **90**, 052104 (2007).